 doi:10.20944/preprints202001.0280.v1

Knockout of the murine ortholog to the human 9p21 coronary artery disease locus leads to SMC proliferation, vascular calcification, and advanced atherosclerosis

Yoko Kojima, MD, PhD[1], Jianqin Ye, MD, PhD[1], Vivek Nanda, PhD[1], Ying Wang, PhD[1], Alyssa M. Flores, BS[1], Kai-Uwe Jarr, MD[1], Pavlos Tsantilas, MD[1], Liang Guo, PhD[2], Aloke V. Finn, MD[2], Renu Virmani, MD[2], and Nicholas J. Leeper, MD[1,3]

[1] Department of Surgery, Division of Vascular Surgery, Stanford University School of Medicine, Stanford, California, USA.

[2]CVPath Institute, Gaithersburg, Maryland, USA.

[3] Department of Medicine, Division of Cardiovascular Medicine, Stanford University School of Medicine, Stanford, California, USA.

Corresponding author:

Nicholas J. Leeper, MD

Divisions of Vascular Surgery and Cardiovascular Medicine

Stanford University

300 Pasteur Drive, Alway Room M103B

Stanford, California 94305

e-mail: nleeper@stanford.edu

Tel/Fax: 650 724 8475 / 650 498 6044

Keywords: Atherosclerosis, Vascular Biology, Calcification, Genetics, 9p21

Preprints (www.preprints.org) | NOT PEER-REVIEWED | Posted: 24 January 2020 doi:10.20944/preprints202001.0280.v1

Abstract:

Background: Genome-wide association studies have identified the chromosome 9p21 locus as one of the most important genetic risk factors for cardiovascular disease. However, the mechanism by which this locus promotes disease remains unclear due to difficulty identifying the causal genes and lack of a suitable animal model.

Methods and Results: A total of 180 coronary artery autopsy specimens were analyzed histopathologically. The genotype of 9p21 (rs1333049) was not associated with any coronary risk factors nor the vulnerable plaque phenotype, but carriers of 9p21 risk allele did demonstrate more lesional calcification. To extend these studies into an animal model, mice with a targeted deletion of the orthologous 70-kb non-coding interval on chromosome 4 (chr4$^{\Delta 70kb/\Delta 70kb}$) were bred onto *ApoE*$^{-/-}$ and fed with high fat diet. Targeted deletion of the 9p21 risk interval increased susceptibility to atherosclerotic plaque progression, but did not affect plaque rupture in the tandem stenosis model. Coronary risk factors such as body weight, blood pressure, lipid, and glucose levels did not differ between genotypes. Von Kossa staining revealed that chr4$^{\Delta 70kb/\Delta 70kb}$, *ApoE*$^{-/-}$ developed more calcification in the plaque compared with chr4$^{+/+}$, *ApoE*$^{-/-}$ mice, and that this this change was accompanied by increased aortic mRNA expression of *Runx2*, a key osteogenic transcription factor. Primarily cultured smooth muscle cells from chr4$^{\Delta 70kb/\Delta 70kb}$ were hyperproliferative, and showed a calcification-prone phenotype after exposure to high-phosphate medium. Treatment with Palbociclib, a selective inhibitor of cyclin-dependent kinase 4/6, reduced mRNA expression of osteogenic genes in smooth muscle cells.

Conclusion: Results from human and mouse studies indicate that the 9p21 non coding risk interval is associated with larger atherosclerotic plaque burden, but not with plaque rupture. 9p21 may promote lesion expansion by inducing the proliferation of de-differentiated and osteogenic smooth muscle cells.

 doi:10.20944/preprints202001.0280.v1

Introduction:

Atherosclerotic cardiovascular disease remains the world's leading killer. Traditional risk factors such as smoking, hypertension and dyslipidemia account for approximately 50% of an individual's lifetime risk for coronary artery disease (CAD). The remaining risk is attributed to a combination of environmental exposures and poorly defined genetic factors. The genome-wide association study (GWAS) approach has been used to identify the loci responsible for the heritable component of CAD. In a series of landmark studies which have now been replicated in over one million individuals, single nucleotide polymorphisms at the chromosome 9p21 locus have been unequivocally implicated as the most significant genetic variants associated with CAD. Despite more than a decade of fine-mapping, molecular genetics and mechanistic studies, the mechanism by which this locus causes disease remains a subject of significant debate. This is largely due to the fact that the disease-associated variants at 9p21 reside in a non-coding region of the genome, and the causal gene(s) responsible for disease have been difficult to definitively identify. Leading hypotheses include the concept that variants at 9p21 alter the expression of a long noncoding RNA known as *ANRIL*, and that this gene may inhibit the transcription of a nearby tumor suppressor gene known as *CDKN2A* and *CDKN2B* [1, 2]. To date, however, conflicting data have been reported and translation of this top GWAS locus has proven surprisingly difficult.

Previously, Pennachio and colleagues generated a mouse deficient in the human 9p21 ortholog by knocking out the entire syntenic region at chromosome 4qC4/5 [3]. This mouse was shown to have markedly reduced expression of the cell cycle regulators, *Cdkn2a* and *Cdkn2b*, and demonstrated a phenotype in which its vascular smooth muscle cells (SMCs) were hyperproliferative and resistant to senescence. However, this animal has not yet been studied on an atherosclerotic background, and the mechanism by which the murine 9p21 ortholog might promote atherogenesis has not yet been described. In the brief report that follows, we report the impact of knocking out the 9p21 locus on cardiovascular disease, highlighting the role of this locus on SMC de-differentiation and acquisition of disease-related phenotypes.

Preprints (www.preprints.org) | NOT PEER-REVIEWED | Posted: 24 January 2020 doi:10.20944/preprints202001.0280.v1

Methods:

Animal model

Chr4$^{\Delta 70kb/+}$ mice were purchased from Jackson Laboratories. Apolipoprotein-E-deficient (*ApoE*$^{-/-}$) mice on a 129 background [4] were kindly gifted by Professor Nobuyo Maeda (University of North Carolina at Chapel Hill, USA) and bred to chr4$^{\Delta 70kb/+}$ mice to generate double knockout mice. PCR detection was performed for mouse genotype using the following primers:

***Chr4* genotyping**:	T7	CGTAATACGACTCACTATAGGGCG
	CHD5'arm.fwd	TATGAAAGCACACTTGTGGGCGTGT
	CHDp3.fwd	AAGGTATCCTAAATACTGTCTTCTTGCAG
	CHDp3.rev	CGAGTCAATTTTCTTCATGTTTATCCTCCA
***ApoE* genotyping**:	oIMR0180	GCCTAGCCGAGGGAGAGCCG
	oIMR0181	TGTGACTTGGGAGCTCTGCAGC
	oIMR0182	GCCGCCCCGACTGCATCT

Genotype was confirmed as follows: chr4$^{+/+}$: 180 bp; Chr4 $^{\Delta 70kb\ /\ \Delta 70kb}$: 236 bp; *ApoE*$^{+/+}$: 155 bp, *ApoE*$^{-/-}$: 245bp.

To evaluate their susceptibility to atherosclerotic plaque development, the mice were initiated on Western diet (21% anhydrous milk fat, 19% casein, and 0.15% cholesterol; catalog # 101511, Dyets Inc.) at 6 weeks of age and maintained on this for 13 or 20 additional weeks. To evaluate plaque vulnerability, we performed tandem stenosis ligations of the carotid artery in the 13 weeks high fat diet cohort, as previously described [5]. Briefly, mice were initiated on high-fat Western diet at 6 weeks of age, and then a tandem stenosis with 150 µm outer diameter was applied to the right carotid artery at 12 weeks of age. After an additional 7 weeks of Western diet (13 total weeks of high fat diet), the animals were euthanized and analyzed for plaque burden in the aortic sinus and intraplaque hemorrhage (IH) in the ligated carotid artery.

Blood pressure was measured by tail cuff method (Kent scientific Corporation, CT) in conscious mice. Tail bleeding assay was performed as previously described [6]. Sterile water and food were available ad libitum. Mice were maintained in a temperature-controlled (20-22 °C) environment with a 12-hour light-dark cycle. All animal studies were approved by the Stanford University Administrative Panel on Laboratory Animal Care (protocol 27279) and conformed to the NIH guidelines for the care and use of laboratory animals.

Tissue preparation and histological analysis

Prior to sacrifice, the mice were fasted overnight. Blood samples were collected via left ventricular cardiac puncture, the mice were perfused with PBS under physiological pressure, and then the aortic

Preprints (www.preprints.org) | NOT PEER-REVIEWED | Posted: 24 January 2020 doi:10.20944/preprints202001.0280.v1

root, arch and branch vessels (including the brachiocephalic, right and left carotid arteries) were meticulously dissected out. Photographs of the aortic arch, brachiocephalic, carotid arteries were captured with a digital camera mounted on a Nikon stereomicroscope to analyze IH. Tissue samples for histological analysis were fixed with 4% paraformaldehyde and embedded in OCT. The descending aorta, hearts, and kidneys were snap-frozen for RNA analysis. Automated hematology was performed on the Sysmex XT-2000 analyzer. Serum cholesterol, triglyceride, glucose levels were measured via a Siemens Dimension Xpand analyzer at the Stanford Animal Diagnostic Laboratory.

For quantification of the aortic root atherosclerotic plaque size, the tissue samples were sectioned at 7-µM thickness, and four sections at 100-µM intervals were stained with Oil red O. The lesion size was measured with Adobe Photoshop CS6 in a blinded manner. Serial sections were stained with Masson's Trichrome (Richard-Allan) and Von Kossa (Polysciences). Immunostaining was performed using Mac3 antibody (BD Pharmingen, 550292, 1:100) and Calponin antibody (Abcam, ab46794, 1:300).

Cell culture studies

Primary mouse vascular SMCs were isolated from the aortae of chr4$^{+/+}$ and chr4$^{\Delta 70kb/\Delta 70kb}$ mice. Briefly, mice were euthanized and perfused with Hank's Balanced Salt solution (HBSS) via left ventricular puncture, then aorta was exposed and dissected carefully from any surrounding tissues. The cleaned aorta was incubated with enzyme solution (HBSS containing 2 units/ml LiberaseTM (Roche) and 2 units/ml Elastase (Worthington)) at 37 °C for 10-15 minutes. After washing with HBSS, the adventitia layer was stripped from the medial layer using 2 fine forceps, chopped into small pieces with fine scissors, and digested in the enzyme solution at 37 °C for 30-40 minutes. Thereafter, the supernatant was removed by centrifugation and the cells were cultured in DMEM supplemented with 10% FBS, 100 units/mL penicillin and 100 µg/mL streptomycin. Experiments were performed on cells up to passage 7. Human coronary artery SMCs were purchased from Lonza (CC-2583) and cultured in SmBM^{TM} Basal Medium containing SmGM^{TM}-2 Supplement Pack (Lonza).

Gene expression analysis

Total RNA was isolated from frozen murine tissue or cultured SMCs by Trizol (Thermo Fisher), cDNA was synthesized with Multiscribe reverse transcriptase (Applied Biosystems), and quantitative reverse-transcription PCR (qPCR) was performed on the ABI PRISM 7900HT with commercially available Taqman probes (Applied Biosystems). Expression of target genes were normalized to the expression of the housekeeping gene, *Gapdh*. The assay IDs of Taqman probes used in this paper were listed below,

Cdkn2a (p16)	Mm00494449_m1
Cdkn2a (p19)	Mm01257348_m1
Cdkn2b	Mm00483241_m1
CD68	Mm03047343_m1
Gapdh	Mm99999915_g1
Ly6a	Mm00726565_m1
Mtap	Mm01257900_m1
Nos2	Mm00440502_m1

Preprints (www.preprints.org) | NOT PEER-REVIEWED | Posted: 24 January 2020 doi:10.20944/preprints202001.0280.v1

Runx2	Mm00501584_m1
Sox9	Mm00448840_m1
Tagln	Mm00441660_m1
Tnf	Mm00443258_m1
ALP	Hs01029144_m1
BMP2	Hs00802901_m1
CDKN2A	Hs00923894_m1
CDKN2B	Hs00793225_m1
GAPDH	Hs01047973_m1
RUNX2	Hs01047973_m1

MTT assay

Mouse aortic SMCs were plated in 96-well plates at a density of 4,000 cells per well, grown at 37 °C overnight, and serum-starved for 24 hours. The cells were stimulated with 10% FBS for 48 hours and cell proliferation was assessed by CellTiter 96 Non-Radioactive Cell Proliferation Assay (Promega), according to the manufacturer's instruction.

In vitro calcification study

Aortic SMCs were seeded in 24-well (50,000 cells per well) or 48-well (25,000 cells per well) plates and grown to confluent monolayers. The cells were cultured in DMEM containing 2.6 mM inorganic phosphate or 10 mM β-glycerol phosphate, 50 µg/mL ascorbic acid, and 100 nM dexamethasone to induce calcification. After 7 days, the cells were washed with PBS, fixed in 4% paraformaldehyde, washed with diH2O, and stained with 2% Alizarin Red S (Sigma-Aldrich, pH 4.2) for 40 minutes at room temperature. The dye solution was removed and the cells were washed with diH2O. Images were taken by a digital camera mounted on a Nikon stereomicroscope. After removal of excess of water, the cells were incubated with 200 µl of 10% acetic acid at room temperature for 10 minutes for quantification of Alizarin red content. The cells were collected using a cell scraper, vortexed for 30 seconds, heated at 85 °C for 10 minutes, then centrifuged at 20,000g for 15 minutes. The supernatant was transferred to a 96-well plate and absorbance at 405 nm was measured by a SpectraMax 190 Microplate Reader (Molecular Devices).

Human samples

A total of 295 human coronary atherosclerotic plaques dissected from 181 male and 32 female victims of sudden cardiac death were sent to the Cardiovascular Pathology Institute (Gaithersburg, Maryland) for autopsy evaluation. Briefly, DNA was extracted from each sample using a Gentra Puregene Tissue Kit or QIAamp DNA FFPE Tissue Kit (Qiagen) according to the manufacturer's instruction. Genotyping for rs1333049 was performed with a Taqman SNP allelic discrimination genotyping assay (Life Technologies 4351379) on an Applied Biosystem 7500 Fast Real-Time polymerase Chain Reaction System [7]. The coronary arteries were serially sectioned at 3-4 mm intervals and processed for histological examination

 doi:10.20944/preprints202001.0280.v1

by hematoxylin and eosin as well as Movat pentachrome. Atherosclerotic plaques were classified as described previously [8, 9]. Briefly, a vulnerable plaque (thin-cap fibroatheroma (TCFA)) was defined as a lesion that was infiltrated by macrophages and had a thin fibrous cap. A ruptured plaque (PR) was defined by the presence of an acute luminal thrombus connected to a lipid-rich necrotic core through a disruption of a thin fibrous cap. A stable plaque (fibroatheroma (FA)) was defined as a plaque with a mature necrotic core covered by a thick fibrous cap rich in SMC or healed plaque rupture. All histomorphometric quantifications were performed in a blinded fashion and locked into a database before performing genotyping and data analysis. Collection, storage, and use of tissue and patient data were performed in agreement with institutional ethical guidelines.

Statistical analysis

Data are expressed as mean ± SEM. Outliers were identified using ROUT analysis. Gaussian distribution was examined by a D'Agostino-Pearson or Shapiro-Wilk test. In experiments where 2 groups were compared, two-tailed Student's t-tests were performed for parametric data and the Mann-Whitney U test was performed for non-parametric data. When comparing multiple groups, data were analyzed by one way ANOVA followed by post-hoc testing (for parametric data) or Kruskal-Wallis test (for non-parametric data). A P value <0.05 was considered to indicate statistical significance. Statistical analyses were performed using GraphPad Prism 8 (GrahPad Inc.).

Preprints (www.preprints.org) | NOT PEER-REVIEWED | Posted: 24 January 2020 doi:10.20944/preprints202001.0280.v1

Results:

We analyzed human coronary artery samples dissected from the hearts of victims of sudden cardiac death. Among the 98 individual genotyped in the autopsy cohort, 34 had ancestral allele (G/G) only, 28 were found to be homozygous for the 9p21 risk allele rs1333049 (C/C), and 36 were heterozygous (C/G). A total of 180 plaques (55 from G/G, 79 from C/G, 46 from C/C) were analyzed. Phenotype of plaque rupture (Erosion+Ruptured) was found in 36% of G/G, 41% of C/G, and 45% of C/C group. Lesion phenotype did not differ between genotype (Fig A, top). In addition, we did not observe any features of lesion instability, including no increase in macrophage infiltration, necrotic core size, or fibrous cap thinning (Suppl Fig 1A). Calcification was found to be significantly higher in the carriers of the risk allele than those of the ancestral allele (Fig A, bottom). This trend was detected across the spectrum of lesion phenotypes and the difference remained significant even after controlling for lesion size. Taken together, these finding suggested that 9p21 risk allele is irrelevant to stable/unstable plaque phenotype, but affect calcification in atherosclerotic plaque.

Deletion of the CAD risk interval accelerates atherosclerosis, without inducing plaque rupture

Chr4 $^{\Delta 70kb/\ \Delta 70kb}$ mice are on 129 genetic background that is less susceptible strain to atherosclerosis [10], and the original report showed that chr4 $^{\Delta 70kb/\ \Delta 70kb}$ mice fed with high-fat high-cholesterol diet for 20 weeks developed small fatty lesion formation equivalent to those in wild type controls of 129Sv background [3]. To further evaluate atherosclerotic lesion development, chr4$^{+/\Delta 70kb}$ mice were bred onto *ApoE*$^{-/-}$ on 129S background and fed with a high fat diet for 13 or 20 weeks. The *ApoE*$^{-/-}$ on 129S background is known to showed slightly different phenotype in hyperlipidemia, atherosclerosis, and vascular calcification compared to widely used *ApoE*$^{-/-}$ on C57BL/6 background [4, 11]. The atherosclerotic lesion size in aortic root was significantly larger in chr4$^{\Delta 70kb\ /\Delta 70kb}$, *ApoE*$^{-/-}$ mice compared with chr4$^{+/+}$, *ApoE*$^{-/-}$ mice (Fig 1B). Deletion of CAD risk interval increased the plaque size in male mice by 33% after 13 weeks high fat diet and by 65% after 20 weeks high fat diet. Heterozygous deletion of CAD risk locus showed intermediate phenotype indicating that there was a gene-dose effect. In contrast to *ApoE*$^{-/-}$ on C57BL/6 background in which female mice develop larger lesion compared with male mice, no significant difference of lesion size was detected between male and female as previously shown. The increase of plaque size by deletion of CAD risk interval was confirmed in female mice as well. The mRNA expression of inflammatory markers were upregulated in descending aorta from chr4$^{\Delta 70kb\ /\Delta 70kb}$, *ApoE*$^{-/-}$ (Suppl Fig 1B). Histological analysis revealed that the atherosclerotic plaque of chr4$^{\Delta 70kb\ /\Delta 70kb}$, *ApoE*$^{-/-}$ did not show any unstable disease phenotype such as larger necrotic core size, decreased collagen content, or increased macrophage infiltration compared to *ApoE*$^{-/-}$ mice (Supp Fig 1C, 1D). To further investigate the effect on plaque stability, we analyzed plaque rupture model of carotid arteries applied tandem stenosis which showed characteristics typically seen in human unstable plaques. IH was found in 58% of *ApoE*$^{-/-}$, 65% of chr4$^{+/\ \Delta\ 70kb}$, *ApoE*$^{-/-}$, and 60% of chr4$^{\Delta 70kb\ /\Delta 70kb}$, *ApoE*$^{-/-}$mice and there was no difference between genotypes, indicating that deletion of CAD risk interval had no effect on plaque rupture (Fig C). Unlike the previous data from the normal chow fed chr4$^{\Delta 70kb\ /\Delta 70kb}$ mice, there was no significant difference of body weight in both gender and time point (Suppl Fig 1E). In addition, we did not find the increased mortality in chr4$^{\Delta 70kb\ /\Delta 70kb}$, *ApoE*$^{-/-}$ on Western diet (data not shown). Other CAD risk factors such as blood pressure, fasting glucose, and serum lipid levels did not differ between genotypes (Suppl

Preprints (www.preprints.org) | NOT PEER-REVIEWED | Posted: 24 January 2020 doi:10.20944/preprints202001.0280.v1

Fig 1F,1G). Since knockdown of *Cdkn2a* expression on LDL receptor knockout mice were reported to show enhanced megakaryopoiesis and platelet activity [12], we measured complete blood counts (CBCs) and tail bleeding time on chr4 $^{\Delta 70kb/\Delta 70kb}$, *ApoE*$^{-/-}$mice. No significant difference was observed in platelet count, platelet distribution width, mean platelet volume, percentage of large platelet, platelet-crit, or tail bleeding time between *ApoE*$^{-/-}$ and chr4$^{\Delta 70kb/\Delta 70kb}$, *ApoE*$^{-/-}$ mice (Suppl Fig 2A).

The reduction of *Cdkn2a* and *Cdkn2b* expression was reported in the heart and aorta [13] from normolipidemic chr4 $^{\Delta 70kb/\Delta 70kb}$ mouse. We measured the mRNA expression of the genes in the heart, kidney, and atherosclerotic aortic tissues from the mice fed with Western diet. As expected, *p16* and *p15* in the heart was significantly decreased in chr4$^{\Delta 70kb/\Delta 70kb}$, *ApoE*$^{-/-}$ mice compared to *apoE*$^{-/-}$ (Suppl Fig 2B). In the atherosclerotic aorta, *p19* and *p15* expression was decreased (Suppl Fig 2C). Von kossa staining revealed that calcification area in the neointima was significantly increased in chr4$^{\Delta 70kb/\Delta 70kb}$, *ApoE*$^{-/-}$, as with human carrying risk allele. (Fig D).

To understand the mechanisms how deletion of CAD risk interval increased atherosclerotic plaque burden, we performed in vitro assays using primary cultured vascular SMCs. The proliferation rate of vascular SMCs from chr4$^{\Delta 70kb/\Delta 70kb}$ was increased compared with those from chr4$^{+/+}$ mice as previously described (Fig 2A). The expression of *Runx2*, an important osteogenic transcription factor, was increased by 2-fold in the aorta from in chr4$^{\Delta 70kb/\Delta 70kb}$, *ApoE*$^{-/-}$, whereas SMC marker, *Transgelin* expression was decreased (Fig F, top left). Interestingly, chondrogenic marker *Sox9* was also upregulated in in chr4$^{\Delta 70kb/\Delta 70kb}$, *ApoE*$^{-/}$. The similar result was observed in primary cultured SMC isolated from chr4$^{\Delta 70kb/\Delta 70kb}$ (Fig F, top right). Alizarin red staining confirmed increased calcification in chr4$^{\Delta 70kb/\Delta 70kb}$ SMCs after exposure to inorganic phosphate or osteogenic medium. Because vascular SMCs from human carrying the 9p21 risk allele are known to have reduced expression of CDK inhibitor, [14], we treated SMCs with Palbociclib, a specific inhibitor of CDK4/6, and found that this agent prevented the upregulation of calcification markers in SMCs.

 doi:10.20944/preprints202001.0280.v1

Discussion:

Thus far, efforts aimed at explaining how the top GWAS locus causes cardiovascular disease have been underwhelming. Many groups, including ours, have knocked out individual candidate genes in murine models of atherosclerosis, and diverging results have been reported. This may be due to the fact that there is remarkable compensation of genes near the 9p21 locus, and several groups have found that knockout of one gene (e.g. *Cdkn2b*) is accompanied by a concomitant increase of another (e.g. *Cdkn2a* or its splice variant, *Arf*), making it difficult to faithfully model the human condition. Therefore, the introduction of a mouse atherosclerosis model deficient in the entire 9p21 ortholog is important, as it may be more reflective of the what is occurring in the ~50% of individuals in the United States who carry this very important risk allele.

In keeping with the large body of published epidemiological research [15-17], we found that 9p21 has no impact whatsoever on traditional risk factors. Our mice had no differences in blood pressure, lipid levels, or insulin resistance, confirming that the 9p21 locus promotes disease via an orthogonal mechanism which is not addressed with currently available therapies. Instead, we confirm that mice deficient in the 9p21 ortholog have a simultaneous reduction in *Cdkn2a* and *Cdkn2b*, two key tumor suppressor genes that regulate cellular differentiation status and replicative capacity. We find that SMCs from the 9p21 KO mouse are predisposed to 'de-differentiate' and assume a macrophage-like (data not shown) and osteogenic status. We found that 9p21-deficient cells expressed higher levels of the key calcification gene Runx2 and had accelerated ossification in an ex vivo calcification model.

A question which has been debated amongst the GWAS community is whether the 9p21 locus merely increases plaque burden, or if it also accelerates lesion instability and propensity for plaque rupture. Using a tandem-stenosis plaque rupture model, we failed to observe an increase in intraplaque hemorrhage in mice deficient in the 9p21 ortholog. These data corroborate prior human studies [18, 19], which can be difficult to interpret due to low-resolution phenotyping and the overlap of patients who have both CAD (plaque burden) and myocardial infarction (plaque vulnerability). Herein, we performed careful quantitative histological analysis of human subjects with and without the 9p21 risk allele, and found that the dominant phenotype amongst affected individuals was an increase in lesional calcification. While mechanistic studies are necessary to determine how loss of Cdkn2a/Cdkn2b can accelerate the osteogenic transformation of vascular SMC, it is now well known that coronary calcium burden is a potent predictor of future risk for adverse cardiovascular outcomes. Accordingly, future translational efforts are indicated to determine if carriers of the 9p21 risk allele might benefit from anti-calcification therapy, which could be provided in a 'personalized' manner for those born with this key genetic risk factor.

References:

1. Holdt LM, Teupser D. Long Noncoding RNA ANRIL: Lnc-ing Genetic Variation at the Chromosome 9p21 Locus to Molecular Mechanisms of Atherosclerosis. *Front Cardiovasc Med*. 2018;5:145. doi: 10.3389/fcvm.2018.00145.
2. Holdt LM, Hoffmann S, Sass K, Langenberger D, Scholz M, Krohn K, Finstermeier K, Stahringer A, Wilfert W, Beutner F, et al. Alu elements in ANRIL non-coding RNA at chromosome 9p21 modulate atherogenic cell functions through trans-regulation of gene networks. *PLoS Genet*. 2013;9:e1003588. doi: 10.1371/journal.pgen.1003588.
3. Visel A, Zhu Y, May D, Afzal V, Gong E, Attanasio C, Blow MJ, Cohen JC, Rubin EM, Pennacchio LA. Targeted deletion of the 9p21 non-coding coronary artery disease risk interval in mice. *Nature*. 2010;464:409-412. doi: 10.1038/nature08801.
4. Maeda N, Johnson L, Kim S, Hagaman J, Friedman M, Reddick R. Anatomical differences and atherosclerosis in apolipoprotein E-deficient mice with 129/SvEv and C57BL/6 genetic backgrounds. *Atherosclerosis*. 2007;195:75-82. doi: 10.1016/j.atherosclerosis.2006.12.006.
5. Chen YC, Bui AV, Diesch J, Manasseh R, Hausding C, Rivera J, Haviv I, Agrotis A, Htun NM, Jowett J, et al. A novel mouse model of atherosclerotic plaque instability for drug testing and mechanistic/therapeutic discoveries using gene and microRNA expression profiling. *Circ Res*. 2013;113:252-265. doi: 10.1161/CIRCRESAHA.113.301562.
6. Liu Y, Jennings NL, Dart AM, Du XJ. Standardizing a simpler, more sensitive and accurate tail bleeding assay in mice. *World J Exp Med*. 2012;2:30-36. doi: 10.5493/wjem.v2.i2.30.
7. Nanda V, Downing KP, Ye J, Xiao S, Kojima Y, Spin JM, DiRenzo D, Nead KT, Connolly AJ, Dandona S, et al. CDKN2B Regulates TGFbeta Signaling and Smooth Muscle Cell Investment of Hypoxic Neovessels. *Circ Res*. 2016;118:230-240. doi: 10.1161/CIRCRESAHA.115.307906.
8. Narula J, Nakano M, Virmani R, Kolodgie FD, Petersen R, Newcomb R, Malik S, Fuster V, Finn AV. Histopathologic characteristics of atherosclerotic coronary disease and implications of the findings for the invasive and noninvasive detection of vulnerable plaques. *J Am Coll Cardiol*. 2013;61:1041-1051. doi: 10.1016/j.jacc.2012.10.054.
9. Yahagi K, Kolodgie FD, Lutter C, Mori H, Romero ME, Finn AV, Virmani R. Pathology of Human Coronary and Carotid Artery Atherosclerosis and Vascular Calcification in Diabetes Mellitus. *Arterioscler Thromb Vasc Biol*. 2017;37:191-204. doi: 10.1161/ATVBAHA.116.306256.
10. Paigen B, Ishida BY, Verstuyft J, Winters RB, Albee D. Atherosclerosis susceptibility differences among progenitors of recombinant inbred strains of mice. *Arteriosclerosis*. 1990;10:316-323. doi:
11. Wait JM, Tomita H, Burk LM, Lu J, Zhou OZ, Maeda N, Lee YZ. Detection of aortic arch calcification in apolipoprotein E-null mice using carbon nanotube-based micro-CT system. *J Am Heart Assoc*. 2013;2:e003358. doi: 10.1161/JAHA.112.003358.
12. Wang W, Oh S, Koester M, Abramowicz S, Wang N, Tall AR, Welch CL. Enhanced Megakaryopoiesis and Platelet Activity in Hypercholesterolemic, B6-Ldlr-/-, Cdkn2a-Deficient Mice. *Circ Cardiovasc Genet*. 2016;9:213-222. doi: 10.1161/CIRCGENETICS.115.001294.
13. Loinard C, Basatemur G, Masters L, Baker L, Harrison J, Figg N, Vilar J, Sage AP, Mallat Z. Deletion of chromosome 9p21 noncoding cardiovascular risk interval in mice alters Smad2 signaling and promotes vascular aneurysm. *Circ Cardiovasc Genet*. 2014;7:799-805. doi: 10.1161/CIRCGENETICS.114.000696.
14. Motterle A, Pu X, Wood H, Xiao Q, Gor S, Ng FL, Chan K, Cross F, Shohreh B, Poston RN, et al. Functional analyses of coronary artery disease associated variation on chromosome 9p21 in vascular smooth muscle cells. *Hum Mol Genet*. 2012;21:4021-4029. doi: 10.1093/hmg/dds224.

15. Johnson AD, Hwang SJ, Voorman A, Morrison A, Peloso GM, Hsu YH, Thanassoulis G, Newton-Cheh C, Rogers IS, Hoffmann U, et al. Resequencing and clinical associations of the 9p21.3 region: a comprehensive investigation in the Framingham heart study. *Circulation*. 2013;127:799-810. doi: 10.1161/CIRCULATIONAHA.112.111559.
16. Samani NJ, Erdmann J, Hall AS, Hengstenberg C, Mangino M, Mayer B, Dixon RJ, Meitinger T, Braund P, Wichmann HE, et al. Genomewide association analysis of coronary artery disease. *N Engl J Med*. 2007;357:443-453. doi: 10.1056/NEJMoa072366.
17. McPherson R, Pertsemlidis A, Kavaslar N, Stewart A, Roberts R, Cox DR, Hinds DA, Pennacchio LA, Tybjaerg-Hansen A, Folsom AR, et al. A common allele on chromosome 9 associated with coronary heart disease. *Science*. 2007;316:1488-1491. doi: 10.1126/science.1142447.
18. Dandona S, Stewart AF, Chen L, Williams K, So D, O'Brien E, Glover C, Lemay M, Assogba O, Vo L, et al. Gene dosage of the common variant 9p21 predicts severity of coronary artery disease. *J Am Coll Cardiol*. 2010;56:479-486. doi: 10.1016/j.jacc.2009.10.092.
19. Chan K, Patel RS, Newcombe P, Nelson CP, Qasim A, Epstein SE, Burnett S, Vaccarino VL, Zafari AM, Shah SH, et al. Association between the chromosome 9p21 locus and angiographic coronary artery disease burden: a collaborative meta-analysis. *J Am Coll Cardiol*. 2013;61:957-970. doi: 10.1016/j.jacc.2012.10.051.

Preprints (www.preprints.org) | NOT PEER-REVIEWED | Posted: 24 January 2020 doi:10.20944/preprints202001.0

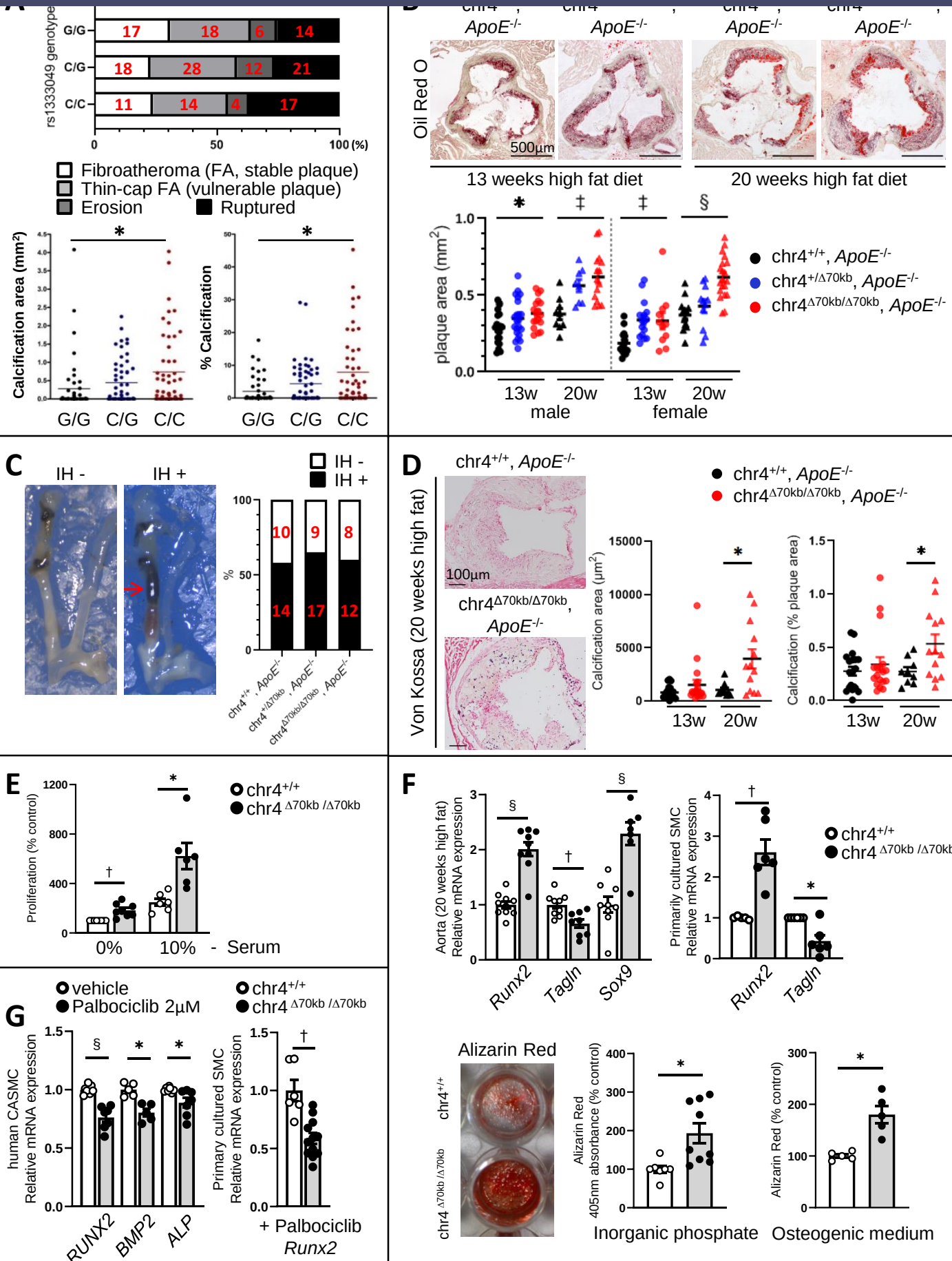

Preprints (www.preprints.org) | NOT PEER-REVIEWED | Posted: 24 January 2020 doi:10.20944/preprints202001.0

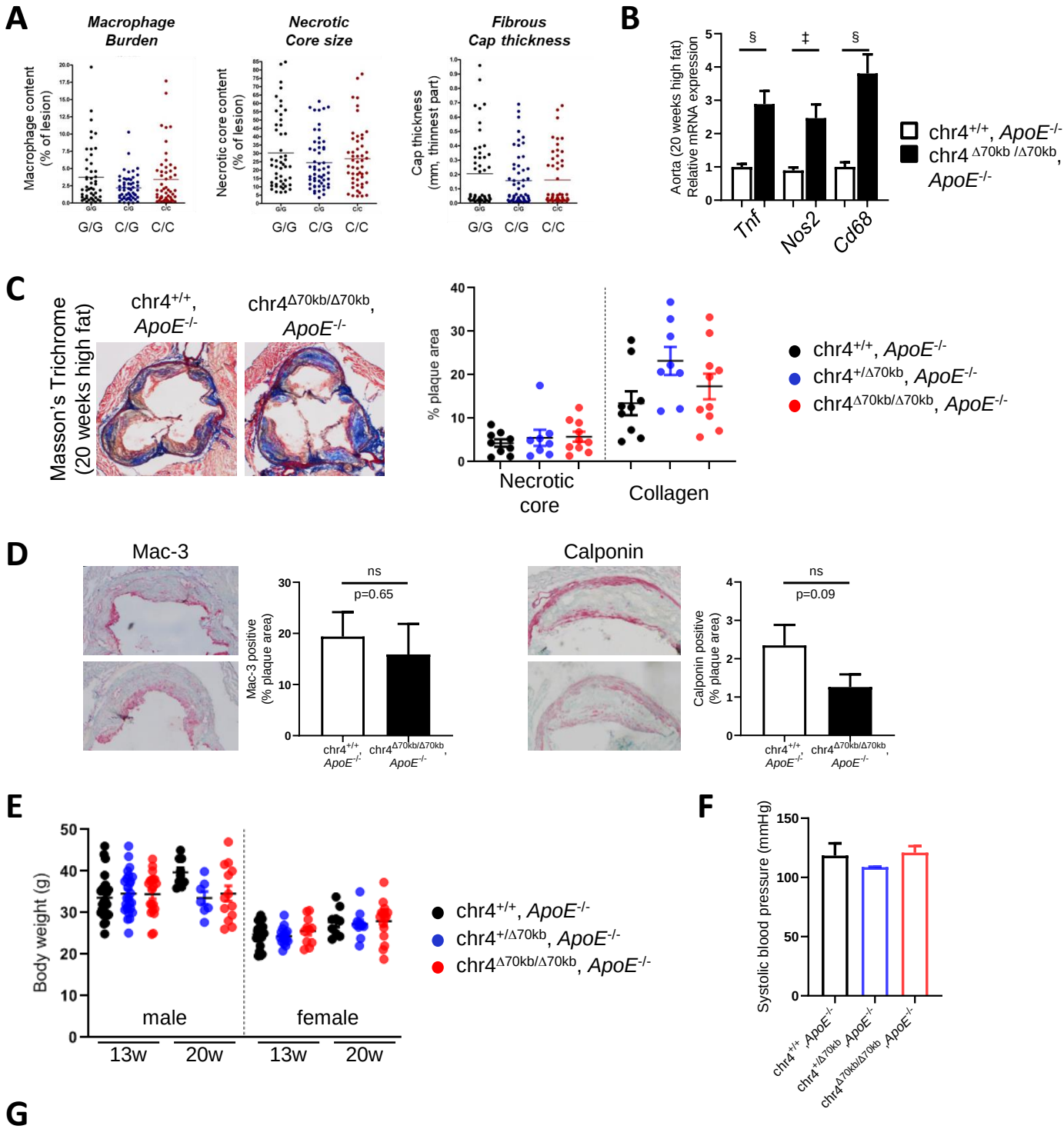

G

	Male			Female		
	chr4$^{+/+}$, *ApoE*$^{-/-}$	chr4$^{+/\Delta 70kb}$, *ApoE*$^{-/-}$	chr4$^{\Delta 70kb/\Delta 70kb}$, *ApoE*$^{-/-}$	chr4$^{+/+}$, *ApoE*$^{-/-}$	chr4$^{+/\Delta 70kb}$, *ApoE*$^{-/-}$	chr4$^{\Delta 70kb/\Delta 70kb}$, *ApoE*$^{-/-}$
Glucose	127.0 ± 31.0	116.0 ± 9.9	70.0 ± 22.0	157.8 ± 23.0	154.5 ± 29.0	113.6 ± 15.2
Cholesterol	828.3 ± 85.5	843.0 ± 177.1	608.0 ± 117.9	919.8 ± 60.2	697.8 ± 185.6	691.2 ± 66.6
Triglyceride	106.5 ±6.89	105.3 ± 22.2	114.5 ± 36.9	75.3 ± 13.5	66.0 ± 12.0	56.2 ± 7.3
LDL cholesterol	500.0 ± 53.8	490.7 ± 82.9	330.8 ± 75.7	558.5 ± 41.7	455.5± 136.7	460.4 ± 33.7

(mg/dL)

Preprints (www.preprints.org) | NOT PEER-REVIEWED | Posted: 24 January 2020 doi:10.20944/preprints202001.0

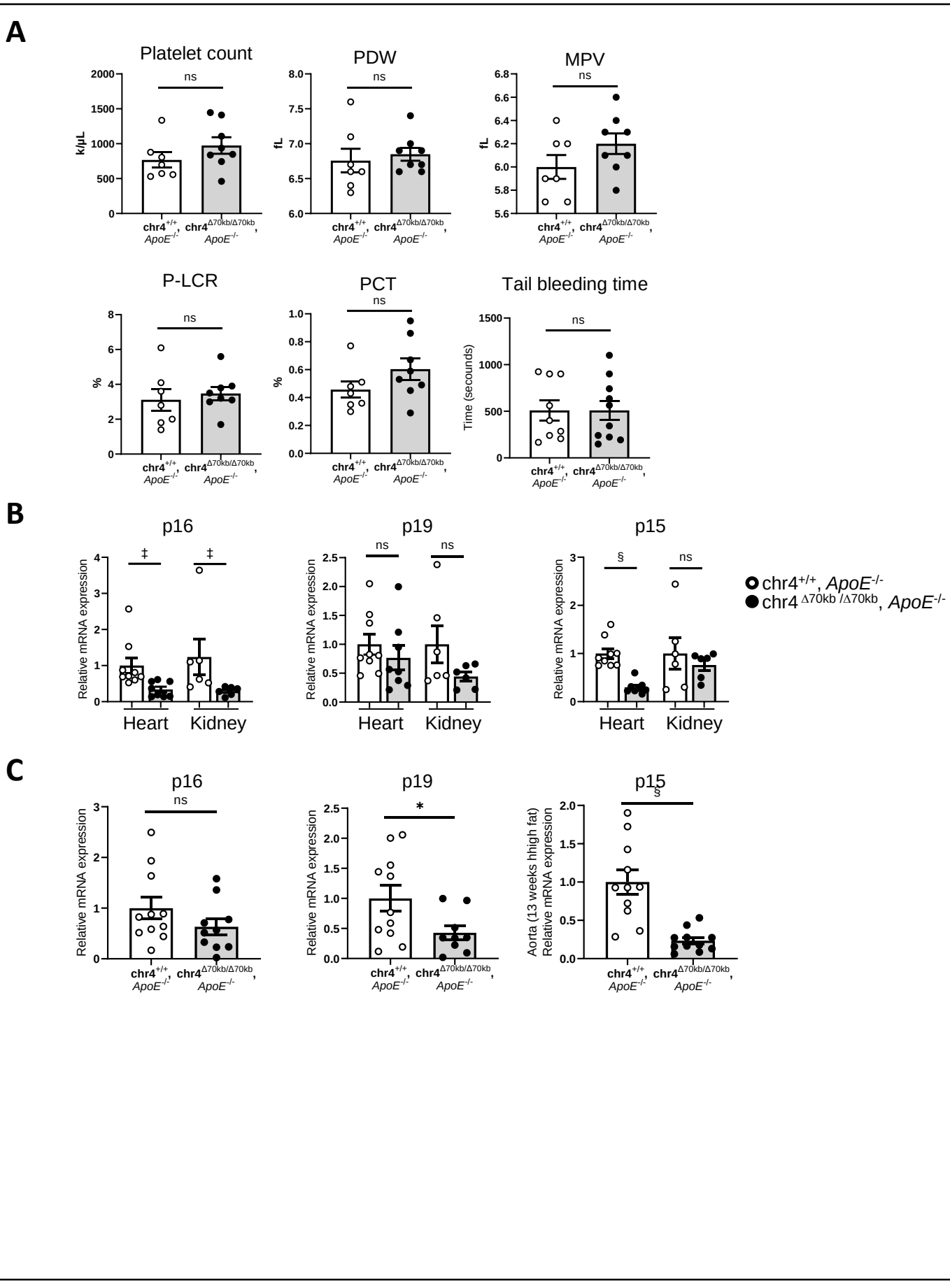

 doi:10.20944/preprints202001.0280.v1

Figure Legend:

A. Human carriers of the 9p21 risk allele develop more calcified, but not more vulnerable atherosclerotic plaques. Numbers in the graph indicate the number of coronary specimens analyzed. **B**. Knockout of the 9p21 locus leads to a significant increase in atherosclerotic burden after 13 or 20 weeks of high fat diet. **C**. Knockout of the 9p21 locus does not increase intraplaque hemorrhage (IH) in the tandem-stenosis plaque rupture model (IH positive example at right). **D**. Von Kossa staining confirms that knockout of the 9p21 locus promotes lesional calcification. **E**. MTT assays reveal that primary-cultured SMCs from chr4$^{\Delta 70kb/\Delta 70kb}$ mice are hyperproliferative. **F**. Knockout of the 9p21 locus induces a calcification phenotype in vivo and vitro, indicated by upregulation of Runx2 and enhanced Alizarin red staining after exposure to 7 days of high-phosphate (left) or osteogenic (right, β-glycerophosphate, ascorbic acid, and dexamethasone) medium. **G**. Palbociclib decreases osteogenic genes in human (left) and mouse (right) SMCs, with disproportionate benefit in cells from chr4$^{\Delta 70kb/\Delta 70kb}$ mice. In vitro experiments were repeated at least 3 times. Data are expressed as mean±SEM. **P*< 0.05, †*P*< 0.01, ‡*P*< 0.005, §*P*< 0.001 via one-way ANOVA or Kruskal-Wallis test, or two-tailed Student's *t* or Mann-Whitney *U* test.

Supplementary Figure1

A. Histological analysis in human coronary artery specimens does not detect the association between plaque vulnerability and rs1333049 status. **B**. qPCR analysis for *Tnf*, *Nos2*, and *Cd68* in in the aortas from the mice fed with Western diet for 20 weeks. **C.** Masson's Trichrome shows no difference of necrotic core size and collagen content in aortic sinus region between genotypes. **D**. Immunohistochemistry for Mac-3 and Calponin shows no difference of macrophage infiltration and a trend towards reduced expression of differentiated SMC in the plaque from chr4$^{\Delta 70kb/\Delta 70kb}$, *ApoE*$^{-/-}$ mice.

 doi:10.20944/preprints202001.0280.v1

E-G. Traditional risk factors of CAD such as body weight (**E**), blood pressure (**F**), and serum lipid and glucose levels (**G**), are similar across genotypes.

Supplementary Figure2

A. CBCs and tail bleeding test shows no significant difference in platelet activity. **B, C**. qPCR analysis for CDK inhibitors in the hearts and kidney (**B**) and aortas (**C**).

References:

1. Holdt LM, Teupser D. Long Noncoding RNA ANRIL: Lnc-ing Genetic Variation at the Chromosome 9p21 Locus to Molecular Mechanisms of Atherosclerosis. *Front Cardiovasc Med*. 2018;5:145. doi: 10.3389/fcvm.2018.00145.
2. Holdt LM, Hoffmann S, Sass K, Langenberger D, Scholz M, Krohn K, Finstermeier K, Stahringer A, Wilfert W, Beutner F, et al. Alu elements in ANRIL non-coding RNA at chromosome 9p21 modulate atherogenic cell functions through trans-regulation of gene networks. *PLoS Genet*. 2013;9:e1003588. doi: 10.1371/journal.pgen.1003588.
3. Visel A, Zhu Y, May D, Afzal V, Gong E, Attanasio C, Blow MJ, Cohen JC, Rubin EM, Pennacchio LA. Targeted deletion of the 9p21 non-coding coronary artery disease risk interval in mice. *Nature*. 2010;464:409-412. doi: 10.1038/nature08801.
4. Maeda N, Johnson L, Kim S, Hagaman J, Friedman M, Reddick R. Anatomical differences and atherosclerosis in apolipoprotein E-deficient mice with 129/SvEv and C57BL/6 genetic backgrounds. *Atherosclerosis*. 2007;195:75-82. doi: 10.1016/j.atherosclerosis.2006.12.006.
5. Chen YC, Bui AV, Diesch J, Manasseh R, Hausding C, Rivera J, Haviv I, Agrotis A, Htun NM, Jowett J, et al. A novel mouse model of atherosclerotic plaque instability for drug testing and mechanistic/therapeutic discoveries using gene and microRNA expression profiling. *Circ Res*. 2013;113:252-265. doi: 10.1161/CIRCRESAHA.113.301562.
6. Liu Y, Jennings NL, Dart AM, Du XJ. Standardizing a simpler, more sensitive and accurate tail bleeding assay in mice. *World J Exp Med*. 2012;2:30-36. doi: 10.5493/wjem.v2.i2.30.
7. Nanda V, Downing KP, Ye J, Xiao S, Kojima Y, Spin JM, DiRenzo D, Nead KT, Connolly AJ, Dandona S, et al. CDKN2B Regulates TGFbeta Signaling and Smooth Muscle Cell Investment of Hypoxic Neovessels. *Circ Res*. 2016;118:230-240. doi: 10.1161/CIRCRESAHA.115.307906.
8. Narula J, Nakano M, Virmani R, Kolodgie FD, Petersen R, Newcomb R, Malik S, Fuster V, Finn AV. Histopathologic characteristics of atherosclerotic coronary disease and implications of the findings for the invasive and noninvasive detection of vulnerable plaques. *J Am Coll Cardiol*. 2013;61:1041-1051. doi: 10.1016/j.jacc.2012.10.054.
9. Yahagi K, Kolodgie FD, Lutter C, Mori H, Romero ME, Finn AV, Virmani R. Pathology of Human Coronary and Carotid Artery Atherosclerosis and Vascular Calcification in Diabetes Mellitus. *Arterioscler Thromb Vasc Biol*. 2017;37:191-204. doi: 10.1161/ATVBAHA.116.306256.
10. Paigen B, Ishida BY, Verstuyft J, Winters RB, Albee D. Atherosclerosis susceptibility differences among progenitors of recombinant inbred strains of mice. *Arteriosclerosis*. 1990;10:316-323. doi:
11. Wait JM, Tomita H, Burk LM, Lu J, Zhou OZ, Maeda N, Lee YZ. Detection of aortic arch calcification in apolipoprotein E-null mice using carbon nanotube-based micro-CT system. *J Am Heart Assoc*. 2013;2:e003358. doi: 10.1161/JAHA.112.003358.
12. Wang W, Oh S, Koester M, Abramowicz S, Wang N, Tall AR, Welch CL. Enhanced Megakaryopoiesis and Platelet Activity in Hypercholesterolemic, B6-Ldlr-/-, Cdkn2a-Deficient Mice. *Circ Cardiovasc Genet*. 2016;9:213-222. doi: 10.1161/CIRCGENETICS.115.001294.
13. Loinard C, Basatemur G, Masters L, Baker L, Harrison J, Figg N, Vilar J, Sage AP, Mallat Z. Deletion of chromosome 9p21 noncoding cardiovascular risk interval in mice alters Smad2 signaling and promotes vascular aneurysm. *Circ Cardiovasc Genet*. 2014;7:799-805. doi: 10.1161/CIRCGENETICS.114.000696.
14. Motterle A, Pu X, Wood H, Xiao Q, Gor S, Ng FL, Chan K, Cross F, Shohreh B, Poston RN, et al. Functional analyses of coronary artery disease associated variation on chromosome 9p21 in vascular smooth muscle cells. *Hum Mol Genet*. 2012;21:4021-4029. doi: 10.1093/hmg/dds224.

15. Johnson AD, Hwang SJ, Voorman A, Morrison A, Peloso GM, Hsu YH, Thanassoulis G, Newton-Cheh C, Rogers IS, Hoffmann U, et al. Resequencing and clinical associations of the 9p21.3 region: a comprehensive investigation in the Framingham heart study. *Circulation*. 2013;127:799-810. doi: 10.1161/CIRCULATIONAHA.112.111559.
16. Samani NJ, Erdmann J, Hall AS, Hengstenberg C, Mangino M, Mayer B, Dixon RJ, Meitinger T, Braund P, Wichmann HE, et al. Genomewide association analysis of coronary artery disease. *N Engl J Med*. 2007;357:443-453. doi: 10.1056/NEJMoa072366.
17. McPherson R, Pertsemlidis A, Kavaslar N, Stewart A, Roberts R, Cox DR, Hinds DA, Pennacchio LA, Tybjaerg-Hansen A, Folsom AR, et al. A common allele on chromosome 9 associated with coronary heart disease. *Science*. 2007;316:1488-1491. doi: 10.1126/science.1142447.
18. Dandona S, Stewart AF, Chen L, Williams K, So D, O'Brien E, Glover C, Lemay M, Assogba O, Vo L, et al. Gene dosage of the common variant 9p21 predicts severity of coronary artery disease. *J Am Coll Cardiol*. 2010;56:479-486. doi: 10.1016/j.jacc.2009.10.092.
19. Chan K, Patel RS, Newcombe P, Nelson CP, Qasim A, Epstein SE, Burnett S, Vaccarino VL, Zafari AM, Shah SH, et al. Association between the chromosome 9p21 locus and angiographic coronary artery disease burden: a collaborative meta-analysis. *J Am Coll Cardiol*. 2013;61:957-970. doi: 10.1016/j.jacc.2012.10.051.